Journal of Dynamics and Differential Equations
https://doi.org/10.1007/s10884-020-09856-1

Global Continuation of Periodic Oscillations to a Diapause Rhythm

Xue Zhang[1] · **Francesca Scarabel**[2] · **Xiang-Sheng Wang**[3] · **Jianhong Wu**[4]

Received: 19 September 2019 / Revised: 20 May 2020

Abstract
We consider a scalar delay differential equation $\dot{x}(t) = -dx(t) + f((1-\alpha)\rho x(t-\tau) + \alpha\rho x(t-2\tau))$ with an instant mortality rate $d > 0$, the nonlinear Rick reproductive function f, a survival rate during all development stages ρ, and a proportion constant $\alpha \in [0, 1]$ with which population undergoes a diapause development. We consider global continuation of a branch of periodic solutions locally generated through the Hopf bifurcation mechanism, and we establish the existence of periodic solutions with periods within $(3\tau, 6\tau)$ for a wide range of parameter values. We show this existence of periodic solutions not only for the delay τ near the first critical value τ^* when a local Hopf bifurcation takes place near the positive equilibrium, but for all $\tau > \tau^*$. We obtain this (global) existence of periodic solutions by using the equivalent-degree based global Hopf bifurcation theory, coupled with an application of the Li–Muldowney technique to rule out periodic solutions with period 3τ. We conduct some numerical simulations to illustrate that this global continuation is completely due to the diapause-delay since solutions of the delay differential equation with only normal development delay in the given biologically realistic range all converge to the positive equilibrium.

Keywords Delay differential equation · Ticks · Diapause · Periodic solution · Global Hopf bifurcation

✉ Jianhong Wu
wujh@mathstat.yorku.ca

Xue Zhang
zhangxue@mail.neu.edu.cn

Francesca Scarabel
francesca.scarabel@helsinki.fi

Xiang-Sheng Wang
xswang@louisiana.edu

1 College of Science, Northeastern University, Shenyang 110819, Liaoning, China

2 Laboratory for Industrial and Applied Mathematics, York University, Toronto, ON M3J 1P3, Canada

3 Department of Mathematics, University of Louisiana at Lafayette, Lafayette, USA

4 Laboratory for Industrial and Applied Mathematics, York University, Toronto, ON M3J 1P3, Canada

Published online: 15 June 2020

Mathematics Subject Classification 34K13 · 34K18 · 92B20

1 Introduction

This modelling study represents a response to the call, from tick ecology and medical entomology community, for "research on diapause phenomena to improve understanding of their biology and of pathogen transmission dynamics" [16]. A number of species of the *Ixodes ricinus* complex of ticks have a worldwide distribution within the northern hemisphere. They act as a vector species responsible for range of tick-borne diseases including Lyme disease, babesiosis, anaplasmosis and tick-borne encephalitis [8]. Ticks have three distinct post-egg stages (larvae, nymphs, and adults), the development from one stage to the next involves a process of host-seeking (questing), attaching, feeding and engorging [14,25]. The hosts providing the blood meals to the ticks are tick-stage dependent with adults feeding on medium-sized and large animals (deer and domestic livestock, for example) and the larval/nymphal ticks parasitizing small to medium-sized mammals (such as rodents) in addition to large animals. In a natural environment, the life cycle is rarely completed in less than 2 years, usually three, and many take as long as 6 years (see [11,16,36] and references therein). Starting from some earlier observation by Milne in 1945 [27] and a series of laboratory and field studies by Belozerov from 1964 [2,3], diapause has been gradually recognized as an important physiological phenomenon and biological strategy for ticks to regulate and suspend development activity during unfavorable environmental conditions in order to ensure the survival.

Here we formulate and analyze a mechanistic model, a scalar delay differential equation, to describe the population dynamics of ticks at a given stage (eggs in our setting). The diapause phenomenon is modelled, and will be illustrated in Sect. 2, by assuming a certain portion of the individuals will undergo a prolonged development during the entire life cycle starting (and ending) at the egg stage, and this assumption leads to incorporation of two time lags one of which for the normal development and another for the prolonged development due to the diapause. Our goal is to examine (1) whether and when diapause may generate oscillatory patterns in a tick population that would exhibit convergence to a positive equilibrium in the absence of diapause; (2) the critical value of portion of ticks undergoing diapause for the oscillation to be generated, in the case when diapause does induce oscillations, and the oscillation frequencies and global continuation when the bifurcation parameter moves away from this critical portion of diapause. We aim to achieve this goal using the S^1-degree theoretical approach based on the work of Erbe et al. [13] and this, as shown in [20], involves a process that (a) identifies bifurcation parameter and determines the critical bifurcation value when the linearization has a pair of purely imaginary eigenvalues; (b) verifies the transversality condition and describes existence, direction and stability of Hopf bifurcations; and (c) establishes bounds for periods of potential periodic solutions and applies the global Hopf bifurcation theory to examine the continuation in the Fuller space.

The identification of a critical bifurcation value for a delay differential equation with two delays is a very challenging problem that has been intensively studied in the literature, see [15,26,31,33–35,37,38] and references therein. Here due to the nature that the developmental and behavioural diapause approximately doubles the normal length of tick life cycle, we are naturally led to the so-called parametric trigonometric functions (see [39]) whose behaviours are amendable to detailed description. The study of Zhang and Wu [39] calculated the first critical bifurcation value by looking at the parametric trigonometric functions on half of their period. In order to identify all bifurcation values (which are needed to apply the global Hopf bifurcation theorem), we will need to describe the behaviours of these parametric trigonometric functions on the entire period, and this will be done in Sect. 3. This description is not only important for the verification of the transversality condition, but also for the determination of the so-called crossing number in the global Hopf bifurcation theorem. The stability of the bifurcated periodic solutions as well as the bifurcation direction can and will be done using the normal form calculation (Sect. 4). Establishing the range of periods of possible periodic solutions is important both for the application of our analyses to tick population dynamics and for applying the global Hopf bifurcation theorem to ensure that the projection of an unbounded connected component of the local Hopf bifurcation in the Fuller space onto the space of periods is bounded, so its projection onto the complementary space is unbounded. Inspired by an early study of Mallet-Paret and Nussbaum [24], we seek to rule out nontrivial periodic solutions of period tripling the normal development delay. Mallet-Paret and Nussbaum achieved this for a delay equation with delayed negative feedback without instantaneous decaying term. Here, in Sect. 5, we will use the Li–Muldowney technique [21] that is based on the Lozinskii measure. Pulling all together, we establish the existence of periodic solutions with periods in a fixed range for a wide range of parameter values. Some numerical simulations will be given in Sect. 6 to illustrate that this global continuation is completely due to the diapause-delay since solutions of the delay differential equation with only normal development delay in the given biologically realistic range converge to the positive equilibrium.

2 Model Formulation

As discussed in the introduction section and as illustrated in Fig. 1, we will consider the following scalar delay differential equation with two time lags

$$\dot{x}(t) = -dx(t) + f((1-\alpha)\rho x(t-\tau) + \alpha\rho x(t-2\tau)), \tag{1}$$

as a model for tick population dynamics in a given region, where $x(t)$ denotes the density of the reproduced eggs at time t, d is the mortality rate, $\rho \in (0, 1)$ is the survival probability from eggs to female egg-laying adults during the development process, and $f(A)$ is the reproductive rate of female egg-laying adults when their density is A. A prototype is given by the Ricker function [29]:

$$f(A) = rAe^{-\sigma A}, \quad A \geq 0, \tag{2}$$

with $r > 0$ for the maximal number of eggs that an egg-laying female can lay per unit time, and $\sigma > 0$ measuring the strength of density dependence.

We should mention that ticks, in their post-egg stages, spend a significant portion of their life cycles off-hosts. During these off-host periods, ticks must contend with a multitude of environmental stresses including prolonged or repeated exposure to desiccating conditions. However, a study [30] shows that when ticks were exposed to continuous dehydration, their survival after 18 weeks of starvation was only minimally impacted. Therefore, we assume throughout the remaining part of this paper, that the tick's survival probability is a constant and independent of the length of the life cycle. Admittedly, tick's survival probability is also highly impacted by severe environmental conditions during the life cycle, and the longer the life cycle the higher the chance of severe environmental conditions to occur during this cycle. Therefore, a modification of the constant survival probability may be justified to account for the decreasing survival probability as the life cycle increases and this will lead to delay

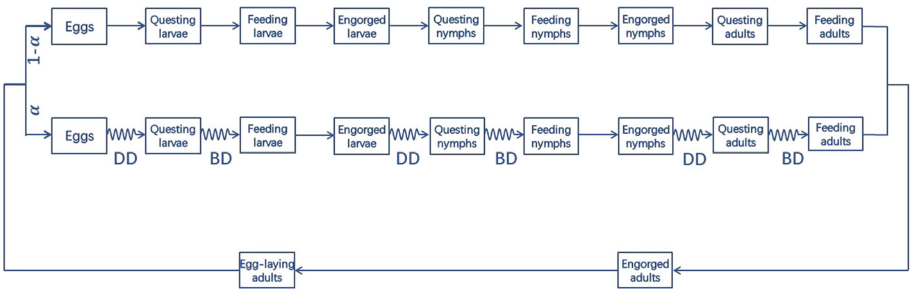

Fig. 1 A schematic illustration of a structured tick population dynamics where a portion $(1-\alpha)$ of eggs experience normal development, through questing larvae, feeding larvae, engorged larvae, questing nymphs, feeding nymphs, engorged nymphs, questing adults to feeding adults, while the remaining portion (α) experience diapause-induction that induces development diapause (DD) and behavior diapause (BD) in the aforementioned development processes. Both portions of ticks will feed the same large-sized mammals (such as deer) and process to the engorged adults, and then develop into egg-laying adults to produce eggs. Diapause can delay host-seeking following the moult, and also delay development of one stage to the next (from eggs to larvae, larva to nymph and from nymph to adult)

differential equations with coefficients depending on the delay, and this should be addressed in future studies.

2.1 Behaviors of Parametric Trigonometric Functions

It is easy to show that model (1), with the function f given by (2), has no positive equilibrium, and $x^* = 0$ is asymptotically stable if $\rho f'(0) < d$. Using the same way as in [39], we can apply the monotone dynamical system theory of [32] to show $x^* = 0$ is indeed global asymptotically stable.

In what follows, we assume

$$\rho f'(0) > d. \tag{3}$$

Then as shown in [39], the equilibrium $x^* = 0$ is unstable and model (1) has one and only one positive equilibrium

$$x_+^* := \frac{1}{\sigma\rho} \ln \frac{\rho f'(0)}{d}, \tag{4}$$

where $f'(0) = r$. In the following, we consider the case $f'(x_+^*) < 0$, i.e.,

$$d < r\rho/e, \tag{5}$$

which guarantees a negative feedback situation around the positive equilibrium x_+^*. This positive equilibrium is asymptotically stable if $\tau \geq 0$ is sufficiently small. To find out the critical value of τ so that x_+^* loses its stability, we linearize model (1) at the equilibrium x_+^* to get a linear equation

$$\dot{x}(t) = -dx(t) + \rho f'(\rho x_+^*)[(1-\alpha)x(t-\tau) + \alpha x(t-2\tau)] \tag{6}$$

with $f'(\rho x_+^*) = \dfrac{d}{\rho}\left(1 - \ln \dfrac{\rho r}{d}\right)$.

Normalizing the delay $\tilde{x}(t) = x(\tau t)$ and dropping $\sim$, we get the linear equation

$$\dot{x}(t) = -\mu x(t) - p[(1-\alpha)x(t-1) + \alpha x(t-2)] \tag{7}$$

with $\mu = d\tau$ and $p = -\rho f'(\rho x_+^*)\tau$.

The characteristic equation of (7) is

$$\lambda = -\mu - p[(1-\alpha)e^{-\lambda} + \alpha e^{-2\lambda}]. \tag{8}$$

If there exists a purely imaginary zero $\lambda = i\omega$ with real $\omega > 0$, then we substitute it into (8) and obtain

$$i\omega = -\mu - p[(1-\alpha)e^{-i\omega} + \alpha e^{-2i\omega}], \tag{9}$$

namely,

$$\begin{cases} -\mu = p \cdot PC_\alpha(\omega), \\ \omega = p \cdot PS_\alpha(\omega), \end{cases} \tag{10}$$

with the parametric trigonometric functions

$$\begin{cases} PC_\alpha(\omega) = (1-\alpha)\cos\omega + \alpha\cos(2\omega), \\ PS_\alpha(\omega) \ = (1-\alpha)\sin\omega + \alpha\sin(2\omega), \end{cases} \tag{11}$$

and

$$PT_\alpha(\omega) = \frac{PS_\alpha(\omega)}{PC_\alpha(\omega)}. \tag{12}$$

The study in [39] depicts the behaviours $PC_\alpha(\omega)$, $PS_\alpha(\omega)$ and $PT_\alpha(\omega)$ in the interval $[0, \pi)$ (half of their periods) when we assume

$$\alpha \geq \max\{-\frac{d}{\rho f'(\rho x_+^*)}, \frac{1}{2}\}. \tag{13}$$

In particular, it is shown that if

$$\begin{aligned} \omega^* &:= \arccos \frac{-(1-\alpha) + \sqrt{(1-\alpha)^2 + 8\alpha(\alpha + \frac{d}{\rho f'(\rho x_+^*)})}}{4\alpha}, \\ \tau^* &:= -\frac{\omega^*}{d \cdot PT_\alpha(\omega^*)}, \end{aligned} \tag{14}$$

then x_+^* is locally asymptotically stable for $\tau \in [0, \tau^*)$ and model (1) undergoes a Hopf bifurcation at $\tau = \tau^*$.

To locate all other Hopf bifurcation values (in addition to τ^*), we need to depict $PC_\alpha(\omega)$ on $[0, 2\pi)$ and to locate all positive values of τ such that

$$PT_\alpha(\omega) = -\frac{\omega}{d\tau}, \tag{15}$$

which is equivalent to

$$\tau = -\frac{\omega}{d \cdot PT_\alpha(\omega)}, \tag{16}$$

for ω satisfying

$$PC_\alpha(\omega) = \frac{d}{\rho f'(\rho x_+^*)}. \tag{17}$$

Lemma 1 *If $\alpha > 1/2$, then there exists no $\omega \in [0, 2\pi)$ such that $PS_\alpha(\omega) = 0$ and $PC_\alpha(\omega) = 0$ hold simultaneously.*

Proof Assume that there exists $\omega \in [0, 2\pi)$ such that $PS_\alpha(\omega) = 0$ and $PC_\alpha(\omega) = 0$ hold simultaneously under the condition $\alpha > \frac{1}{2}$. Then $PS_\alpha(\omega) = 0$ implies that

$$\sin\omega = 0 \quad or \quad \cos\omega = -\frac{1-\alpha}{2\alpha}. \tag{18}$$

Substituting this into

$$PC_\alpha(\omega) = (1-\alpha)\cos\omega + \alpha(2\cos^2\omega - 1) = 0, \tag{19}$$

we can get the following two cases:

(i) $\sin\omega = 0$ and $\alpha + (1-\alpha)\cos\omega = 0$ implying $\alpha = \frac{1}{2}$;
(ii) $-\frac{(1-\alpha)^2}{2\alpha} + \alpha[\frac{2(1-\alpha)^2}{4\alpha^2} - 1] = 0$ implying $\alpha = 0$.

These results above lead to contradictions.

Note that

$$PC'_\alpha(\omega) = -\sin\omega(1-\alpha+4\alpha\cos\omega). \tag{20}$$

Therefore, $PC'_\alpha(\omega) = 0$ if and only if

$$\sin\omega = 0 \quad or \quad \cos\omega = -\frac{1-\alpha}{4\alpha}. \tag{21}$$

That is, in $(0, 2\pi)$, the four zeros of $PC_\alpha(\omega) = 0$ exist in intervals $\left(0, \pi - \arccos\frac{1-\alpha}{4\alpha}\right)$, $\left(\pi - \arccos\frac{1-\alpha}{4\alpha}, \pi\right)$, $\left(\pi, \pi + \arccos\frac{1-\alpha}{4\alpha}\right)$ and $\left(\pi + \arccos\frac{1-\alpha}{4\alpha}, 2\pi\right)$, respectively.

$PC_\alpha(\omega)$ achieves its local maximum and local minimum values at these points as follows:

(i) $PC_\alpha(0) = 1$ is a local maximum;
(ii) $PC_\alpha(\pi - \arccos\frac{1-\alpha}{4\alpha}) = PC_\alpha(\pi + \arccos\frac{1-\alpha}{4\alpha}) = -\frac{(1-\alpha)^2+8\alpha^2}{8\alpha} < 0$ are both local minima;
(iii) $PC_\alpha(\pi) = 2\alpha - 1 > 0$ is a local maximum.

This gives the graph of $PC_\alpha(\omega)$ shown in Fig. 2.
Therefore, we have

Lemma 2 *$PC_\alpha(\omega)$ is symmetrical about $\omega = \pi$ in the interval $[0, 2\pi)$. Moreover, $PC_\alpha(\omega)$ is monotonically increasing in $\left(\pi - \arccos\frac{1-\alpha}{4\alpha}, \pi\right) \cup \left(\pi + \arccos\frac{1-\alpha}{4\alpha}, 2\pi\right)$ and monotonically decreasing in $\left(0, \pi - \arccos\frac{1-\alpha}{4\alpha}\right) \cup \left(\pi, \pi + \arccos\frac{1-\alpha}{4\alpha}\right)$ with the local minimum $-\frac{(1-\alpha)^2+8\alpha^2}{8\alpha}$ achieved at $\pi \pm \arccos\frac{1-\alpha}{4\alpha}$.*

When

$$\frac{\mu}{p} < \frac{(1-\alpha)^2+8\alpha^2}{8\alpha}, \tag{22}$$

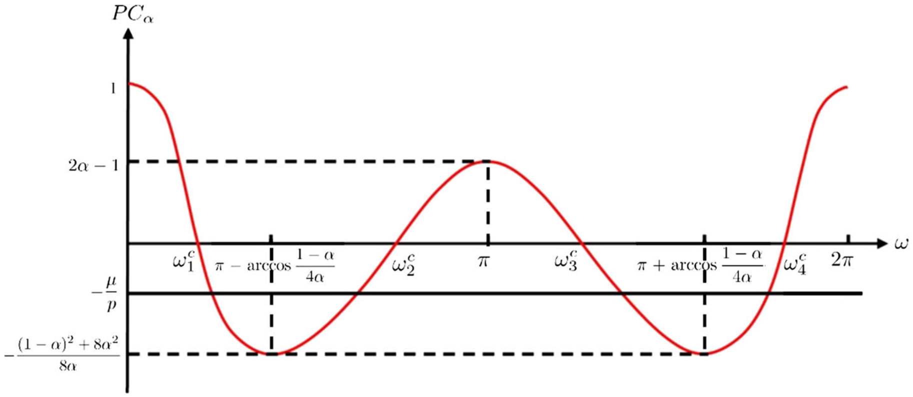

Fig. 2 A schematic illustration of the function $PC_\alpha(\omega)$ with respect to $\omega \in [0, 2\pi)$

$PC_\alpha(\omega) = -\frac{\mu}{p}$ has four solutions $\omega_1, \omega_2, \omega_3, \omega_4 \in [0, 2\pi)$ satisfying

$$0 < \omega_1 < \pi - \arccos\frac{1-\alpha}{4\alpha} < \omega_2 < \pi < \omega_3 < \pi + \arccos\frac{1-\alpha}{4\alpha} < \omega_4 < 2\pi. \tag{23}$$

As $PC_\alpha(\omega)$ is 2π-periodic, we then obtain solutions of

$$PC_\alpha(\omega) = -\frac{\mu}{p} \tag{24}$$

by $\omega_{j,n} = \omega_j + 2n\pi$ for $j = 1, 2, 3, 4$ and $n \geq 0$.

We also note from Lemma 2 that $PC_\alpha(\omega)$ has four zeros $\omega_1^c < \omega_2^c < \omega_3^c < \omega_4^c$ in $(0, 2\pi)$ satisfying

$$0 < \omega_1^c < \omega_1 < \omega_2 < \omega_2^c < \pi < \omega_3^c < \omega_3 < \omega_4 < \omega_4^c < 2\pi. \tag{25}$$

We now consider the monotonicity of $PT_\alpha(\omega)$. From the definition of $PT_\alpha(\omega)$, we obtain

$$\begin{aligned} PT_\alpha'(\omega)PC_\alpha^2(\omega) &= PS_\alpha'(\omega)PC_\alpha(\omega) - PC_\alpha'(\omega)PS_\alpha(\omega) \\ &= (1-\alpha)^2 + 2\alpha^2 + 3\alpha(1-\alpha)\cos\omega \\ &> (1-3\alpha)(1-2\alpha) > 0, \quad \text{as} \quad \alpha > \frac{1}{2}. \end{aligned} \tag{26}$$

Therefore, we have

Lemma 3 *If $\alpha > 1/2$, then $PT_\alpha(\omega)$ is always monotonically increasing in any open interval where it is defined.*

By Lemmas 1 and 2, $PS_\alpha(\omega)$ and $PC_\alpha(\omega)$ can not have zeros at the same time and all zeros of $PC_\alpha(\omega)$ are given by $\omega_1^c < \omega_2^c < \omega_3^c < \omega_4^c$. Therefore, we have the graph of $PT_\alpha(\omega)$ given in Fig. 3.

We can now solve equation $PT_\alpha(\omega) = -\frac{\omega}{\mu}$ for the values of delay

$$\tau = -\frac{\omega}{d \cdot PT_\alpha(\omega)} \tag{27}$$

for every $\omega_{j,n}$, $j = 1, 2, 3, 4$ and $n \geq 0$ as the zeros of

$$PC_\alpha(\omega) = -\frac{\mu}{p} = \frac{d}{\rho f'(\rho x_+^*)}. \tag{28}$$

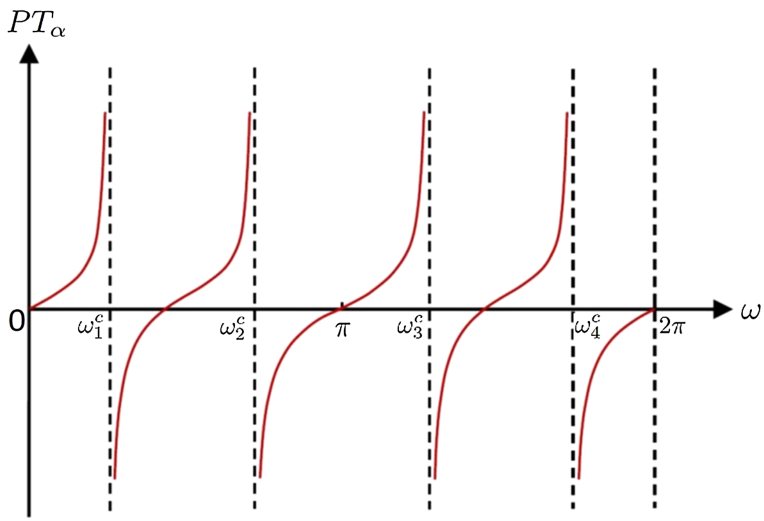

Fig. 3 A schematic illustration of the function $PT_\alpha(\omega)$ with respect to $\omega \in [0, 2\pi)$

We denote those $\omega_{j,n}$, $j = 1, 2, 3, 4$ and $n \geq 0$ satisfying that $PT_\alpha(\omega_{j,n})$ is negative as ω_j^*, $j = 1, 2, \cdots$ in sequence, namely, $\omega_j^* < \omega_{j+1}^*$. It means that such ω_j^* will give a positive value of $\tau_j^* = -\dfrac{\omega_j^*}{d \cdot PT_\alpha(\omega_j^*)}$, $j = 1, 2, \cdots$. Moreover, this procedure establishes the following result:

Theorem 1 *Assume that* (13) *and* (22) *hold. There is a sequence of critical delay* $\tau_j^* < \tau_{j+1}^*$, $j = 1, 2, \cdots$, *for which the characteristic equation* (8) *at* x_+^* *has a pair of purely imaginary zeros* $\pm i\omega_j^*$ *with* $\omega_j^* < \omega_{j+1}^*$, $j = 1, 2, \cdots$.

Remark 1 The first such a critical value of delay is τ^* denoted by τ_α in [39] that corresponds to ω^* in (14).

2.2 Transversality and the Crossing Number

Now, we consider the characteristic function of (1) at the equilibrium x_+^* which takes the following form:

$$\Delta(\Lambda, \tau) = \Lambda + d - \rho f'(\rho x_+^*)[(1-\alpha)e^{-\Lambda\tau} + \alpha e^{-2\Lambda\tau}], \tag{29}$$

where the relationship of eigenvalues between Λ for (29) and λ for (8) is

$$\Lambda = \frac{\lambda}{\tau}. \tag{30}$$

Then we have

$$\Delta(i\frac{\omega_j^*}{\tau_j^*}, \tau_j^*) = 0. \tag{31}$$

Separating the real and imaginary parts, we obtain the following equations:

$$\begin{cases} d = \rho f'(\rho x_+^*)[(1-\alpha)\cos\omega_j^* + \alpha\cos(2\omega_j^*)], \\ \omega_j^* = -\rho f'(\rho x_+^*)\tau_j^*[(1-\alpha)\sin\omega_j^* + \alpha\sin(2\omega_j^*)]. \end{cases} \tag{32}$$

From the first equation of (32), it follows that

$$2\alpha\cos^2\omega_j^* + (1-\alpha)\cos\omega_j^* - (\alpha - \frac{\mu}{p}) = 0, \tag{33}$$

that leads to

$$\cos\omega_j^* = \frac{-(1-\alpha) \pm \sqrt{(1-\alpha)^2 + 8\alpha(\alpha - \frac{\mu}{p})}}{4\alpha}, \tag{34}$$

where μ and p are defined with the same expressions as in (7).

Using the second equation of (32) and the fact that $\omega_j^* > 0$ and $\tau_j^* > 0$, we have

$$\frac{\omega_j^*}{p} = \frac{1}{2}\left[(1-\alpha) \pm \sqrt{(1-\alpha)^2 + 8\alpha(\alpha - \frac{\mu}{p})}\right]\sin\omega_j^*. \tag{35}$$

We can conclude that

Lemma 4 $\cos\omega_j^* \sin\omega_j^* > 0$, *i.e.,* $\cos\omega_j^*$ *and* $\sin\omega_j^*$ *have the same signs for each* ω_j^*.

The partial derivative of (29) with respect to Λ at $i\frac{\omega_j^*}{\tau_j^*}$ and τ_j^* can be expressed as follows

$$\frac{\partial}{\partial\Lambda}\Delta(i\frac{\omega_j^*}{\tau_j^*}, \tau_j^*) = 1 - p[(1-\alpha)\cos\omega_j^* + 2\alpha\cos(2\omega_j^*)] + ip[(1-\alpha)\sin\omega_j^* + 2\alpha\sin(2\omega_j^*)]. \tag{36}$$

Using (34), the imaginary part can be further described as

$$ip[(1-\alpha)\sin\omega_j^* + 2\alpha\sin(2\omega_j^*)] = \pm ip\sqrt{(1-\alpha)^2 + 8\alpha(\alpha - \frac{\mu}{p})}\cdot\sin\omega_j^* \neq 0. \tag{37}$$

Using implicit function theorem, there exists a smooth curve $\Lambda(\tau)$ passing through $(i\frac{\omega_j^*}{\tau_j^*}, \tau_j^*)$ such that

$$\Delta(\Lambda(\tau), \tau) = 0 \tag{38}$$

in some neighborhood of τ_j^*. Differentiating this with respect to τ and substituting $\Lambda = i\frac{\omega_j^*}{\tau_j^*}$ and $\tau = \tau_j^*$, we obtain

$$\begin{aligned}
&\frac{d}{d\tau}\mathrm{Re}(\Lambda)|_{\tau=\tau_j^*} \\
&= \mathrm{Re}\{\frac{-\rho f'(\rho x_+^*)\Lambda((1-\alpha)e^{-\Lambda\tau} + 2\alpha e^{-2\Lambda\tau})}{1 + \rho f'(\rho x_+^*)(1-\alpha)\tau e^{-\Lambda\tau} + 2\rho f'(\rho x_+^*)\alpha\tau e^{-2\Lambda\tau}}\} \\
&= \frac{p\omega_j^*}{\tau_j^{*2}}\frac{((1-\alpha) + 4\alpha\cos\omega_j^*)\sin\omega_j^*}{[1 - p(1-\alpha)\cos\omega_j^* - 2p\alpha\cos(2\omega_j^*))]^2 + p^2[(1-\alpha)\sin\omega_j^* + 2\alpha\sin(2\omega_j^*)]^2}.
\end{aligned} \tag{39}$$

Note that from (34) and Lemma 4, we have

$$\frac{d}{d\tau}\mathrm{Re}(\Lambda)|_{\tau=\tau_j^*} > 0. \tag{40}$$

This establishes the transversality and it is important for the calculation of so-called crossing number at the Hopf bifurcation points with $\tau = \tau_j^*$, $j = 1, 2, \cdots$. We summarize this as

Theorem 2 *There exists a smooth curve $\Lambda(\tau)$ passing each $(i\frac{\omega_j^*}{\tau_j^*}, \tau_j^*)$, $j = 1, 2, \cdots$, that satisfies $\Delta(\Lambda, \tau) = 0$ for τ close to τ_j^* and $Re\Lambda'(\tau_j^*) > 0$.*

Denote by $\tilde{\tau}^*$ and $\pm i\tilde{\omega}^*$ the first critical delay and corresponding to the purely imaginary zeros where a Hopf bifurcation occurs at x_+^* for model (1). Clearly, $\tilde{\tau}^* = \tau^*$ and $\tilde{\omega}^* = \frac{\omega^*}{\tau^*}$. For the purpose of global Hopf bifurcation, we can calculate $\frac{2\pi}{\tilde{\omega}^*\tilde{\tau}^*} \in (3, 6)$ if the following condition is satisfied

$$\alpha < \frac{1}{2} - \frac{d}{\rho f'(\rho x_+^*)}. \tag{41}$$

In the following, we denote by $\tau_J\,(\tau_J = \tau_j^*,\ j = 1, 2, \cdots)$ a generic critical value such that characteristic equation has a pair of purely imaginary zeros $\pm i\omega_J\,(\omega_J = \frac{\omega_j^*}{\tau_j^*},\ j = 1, 2, \cdots)$ and model (1) undergoes a Hopf bifurcation at x_+^*.

3 Bifurcation Direction and Stability: Local Analysis

For the convenience, we introduce the following dimensionless variables

$$\tilde{t} = \tilde{\tau}t, \quad \tilde{\tau} = d\tau, \quad y(\tilde{t}) = \sigma\rho x(\tau t), \tag{42}$$

and rewrite system (1) as

$$\dot{y}(\tilde{t}) = -y(\tilde{t}) + \kappa h((1-\alpha)y(\tilde{t} - \tilde{\tau}) + \alpha y(\tilde{t} - 2\tilde{\tau})), \tag{43}$$

where $\kappa = \rho r/d$ and $h(x) = xe^{-x}$.

Dropping $\sim$ for simplification of notations, system (43) takes the following form

$$\dot{y}(t) = -y(t) + \kappa h((1-\alpha)y(t-\tau) + \alpha y(t-2\tau)). \tag{44}$$

Notice that the positive equilibrium of model (44) is $y_+^* = \sigma\rho x_+^*$. We denote by $\tau_h\,(\tau_h = d\tau_J)$ the critical value of Hopf bifurcation for model (44).

To discuss the directions, stability and period of Hopf bifurcation by the normal form and center manifold theory presented in Hassard et al.[19], we first normalize the delay to system (44) and translate the positive equilibrium y_+^* into the original through introducing

$$z(t) = y(2\tau t) - y_+^*, \tag{45}$$

and then we have

$$\begin{aligned}\dot{z}(t) &= 2\tau[-(z(t) + y_+^*) + \kappa h\left((1-\alpha)(z(t-\frac{1}{2}) + y_+^*) + \alpha(z(t-1) + y_+^*)\right)] \\ &= 2\tau[-z(t) - y_+^* + \left(y_+^* + (1-\alpha)z(t-\frac{1}{2}) + \alpha z(t-1)\right)e^{-((1-\alpha)z(t-\frac{1}{2})+\alpha z(t-1))}].\end{aligned} \tag{46}$$

It is clear to see that the linearization system of model (46) has purely imaginary eigenvalue denoted by $\pm i2\omega_J\tau_J$ here.

Let $\tau_1 = 2\tau_h + \nu$, system (46) can be written as a functional differential equation

$$\dot{z}(t) = L_\nu(z_t) + F(\nu, z_t), \tag{47}$$

where L_ν, F are given, respectively, by

$$L_\nu(\phi) = (2\tau_h + \nu)[-\phi(0) + (1-\alpha)(1-y_+^*)\phi\left(-\frac{1}{2}\right) + \alpha(1-y_+^*)\phi(-1)], \tag{48}$$

$$\begin{aligned} F(\nu, \phi) =& (2\tau_h + \nu)[\frac{1}{2}(1-\alpha)^2(-2+y_+^*)\phi^2\left(-\frac{1}{2}\right) + \alpha(1-\alpha)(-2+y_+^*)\phi\left(-\frac{1}{2}\right) \\ & \cdot \phi(-1) + \frac{1}{2}\alpha^2(-2+y_+^*)\phi^2(-1)] + \frac{1}{6}(1-\alpha)^3(3-y_+^*)\phi^3\left(-\frac{1}{2}\right) \\ & + \frac{1}{2}\alpha(1-\alpha)^2(3-y_+^*)\phi^2\left(-\frac{1}{2}\right)\phi(-1) + \frac{1}{2}\alpha^2(1-\alpha)(3-y_+^*)\phi\left(-\frac{1}{2}\right) \\ & \phi^2(-1) + \frac{1}{6}\alpha^3(3-y_+^*)\phi^3(-1) + \cdots, \end{aligned} \tag{49}$$

where $\phi \in C([-1, 0], \mathbb{R})$. By the Riesz representation theorem, there exists a bounded variation function $\eta(\theta, \nu)$ such that

$$L_\nu\phi = \int_{-1}^{0} d\eta(\theta, \nu)\phi(\theta), \quad \text{for} \quad \phi \in C, \tag{50}$$

where we can choose

$$\eta(\theta, \nu) = \begin{cases} (2\tau_h + \nu)(-1 + (1-\alpha)(1-y_+^*) + \alpha(1-y_+^*)), & \theta = 0, \\ (2\tau_h + \nu)((1-\alpha)(1-y_+^*) + \alpha(1-y_+^*)), & \theta \in [-\frac{1}{2}, 0), \\ (2\tau_h + \nu)\alpha(1-y_+^*), & \theta \in (-1, -\frac{1}{2}), \\ 0, & \theta = -1. \end{cases} \tag{51}$$

Define

$$A(\nu)\phi = \begin{cases} \dfrac{d\phi(\theta)}{d\theta}, & \theta \in [-1, 0), \\ \int_{-1}^{0} d\eta(s, \nu)\phi(s), & \theta = 0, \end{cases} \tag{52}$$

and

$$R(\nu)\phi = \begin{cases} 0, & \theta \in [-1, 0), \\ F(\nu, \phi), & \theta = 0. \end{cases} \tag{53}$$

Then system (47) is equivalent to

$$\dot{z}_t = A(\nu)z_t + R(\nu)x_t, \tag{54}$$

where $z_t(\theta) = z(t+\theta)$ for $\theta \in [-1, 0]$.

For $\psi \in C^1([0, 1], \mathbb{R})$, define an operator

$$A^*\psi(s) = \begin{cases} -\dfrac{d\psi(s)}{ds}, & s \in (0, 1], \\ \int_{-1}^{0} d\eta^T(t, 0)\psi(-t), & s = 0, \end{cases} \tag{55}$$

and bilinear form

$$\langle \psi(s), \phi(\theta) \rangle = \overline{\psi}(0)\phi(0) - \int_{-1}^{0} \int_{\xi=0}^{\theta} \overline{\psi}(\xi - \theta) d\eta(\theta) \phi(\xi) d\xi. \tag{56}$$

where $\eta(\theta) = \eta(\theta, 0)$, $A = A(0)$ and A^* are adjoint operators.

In terms of the discussion mentioned above, we see that $\pm i4\omega_J\tau_J$ are eigenvalues of $A(0)$ and A^*. Let $q(\theta) = e^{i4\omega_J\tau_J\theta}(\theta \in [-1, 0])$ and $q^*(s) = De^{i4\omega_J\tau_J s}(s \in [0, 1])$ be the eigenvectors of $A(0)$ and A^* corresponding to the eigenvalues $i4\omega_J\tau_J$ and $-i4\omega_J\tau_J$, respectively.

It follows from (56) that

$$\begin{aligned} \langle q^*(s), q(\theta) \rangle &= \overline{q}^*(0)q(0) - \int_{-1}^{0} \int_{\xi=0}^{\theta} \overline{q}^*(\xi - \theta) d\eta(\theta) q(\xi) d\xi \\ &= \overline{D}[1 + (1-\alpha)(1 - y_+^*)\tau_h e^{-i2\omega_J\tau_J} + 2\alpha(1 - y_+^*)\tau_h e^{-i4\omega_J\tau_J}] \end{aligned}. \tag{57}$$

Then we have

$$\overline{D} = \left(1 + (1-\alpha)(1 - y_+^*)\tau_h e^{-i2\omega_J\tau_J} + 2\alpha(1 - y_+^*)\tau_h e^{-i4\omega_J\tau_J}\right)^{-1}. \tag{58}$$

using the procedure outlined in Hassard et al. [19], we can compute those important coefficients of $g(z, \overline{z}) = \overline{q}^*(0)F_0(z, \overline{z})$ as follows

$$\begin{aligned} g_{20} &= 2\overline{D}\tau_h(-2 + y_+^*)[(1-\alpha)^2 e^{-i4\omega_J\tau_J} + 2\alpha(1-\alpha)e^{-i6\omega_J\tau_J} + \alpha^2 e^{-i8\omega_J\tau_J}], \\ g_{11} &= 2\overline{D}\tau_h(-2 + y_+^*)[(1-\alpha)^2 + 2\alpha(1-\alpha)Re\{e^{i2\omega_J\tau_J}\} + \alpha^2], \\ g_{02} &= 2\overline{D}\tau_h(-2 + y_+^*)[(1-\alpha)^2 e^{i4\omega_J\tau_J} + 2\alpha(1-\alpha)e^{i6\omega_J\tau_J} + \alpha^2 e^{i8\omega_J\tau_J}], \\ g_{21} &= 4\overline{D}\tau_h\{\frac{1}{2}(1-\alpha)^2(-2 + y_+^*)[2W_{11}(-\frac{1}{2})e^{-i2\omega_J\tau_J} + W_{20}(-\frac{1}{2})e^{i2\omega_J\tau_J}] \\ &\quad + \alpha(1-\alpha)(-2 + y_+^*)[W_{11}(-1)e^{-i2\omega_J\tau_J} + \frac{1}{2}W_{20}(-1)e^{i2\omega_J\tau_J} \\ &\quad + W_{11}(-\frac{1}{2})e^{-i4\omega_J\tau_J} + \frac{1}{2}W_{20}(-\frac{1}{2})e^{i4\omega_J\tau_J}] + \frac{1}{2}\alpha^2(-2 + y_+^*) \\ &\quad \cdot [2W_{11}(-1)e^{-i4\omega_J\tau_J} + W_{20}(-1)e^{i4\omega_J\tau_J}] + \frac{1}{2}(1-\alpha)^3(3 - y_+^*)e^{-i2\omega_J\tau_J} \\ &\quad + \frac{1}{2}\alpha(1-\alpha)^2(3 - y_+^*)(1 + 2e^{-i4\omega_J\tau_J}) + \frac{1}{2}\alpha^2(1-\alpha)(3 - y_+^*) \\ &\quad \cdot (2e^{-i2\omega_J\tau_J} + e^{-i6\omega_J\tau_J}) + \frac{1}{2}\alpha^3(3 - y_+^*)e^{-i4\omega_J\tau_J}\}, \end{aligned} \tag{59}$$

where for $\theta \in [-1, 0]$,

$$\begin{aligned} W_{20}(\theta) &= \frac{ig_{20}}{4\omega_J\tau_h}e^{i4\omega_J\tau_J\theta} + \frac{i\overline{g}_{02}}{12\omega_J\tau_h}e^{-i4\omega_J\tau_J\theta} + R_1 e^{i8\omega_J\tau_J\theta}, \\ W_{11}(\theta) &= -\frac{ig_{11}}{4\omega_J\tau_h}e^{i4\omega_J\tau_J\theta} + \frac{i\overline{g}_{11}}{4\omega_J\tau_h}e^{-i4\omega_J\tau_J\theta} + R_2, \\ R_1 &= 2[i4\omega_J + 1 - (1-\alpha)(1 - y_+^*)e^{-i4\omega_J\tau_J} - \alpha(1 - y_+^*)e^{-i8\omega_J\tau_J}]^{-1}S_1, \\ R_2 &= 2(y_+^*)^{-1}S_2, \\ S_1 &= \frac{1}{2}(-2 + y_+^*)[(1-\alpha)^2 e^{-i4\omega_J\tau_\alpha} + 2\alpha(1-\alpha)e^{-i6\omega_J\tau_J} + \alpha^2 e^{-i8\omega_J\tau_J}], \\ S_2 &= \frac{1}{2}(-2 + y_+^*)[(1-\alpha)^2 + 2\alpha(1-\alpha)Re\{e^{i2\omega_J\tau_J}\} + \alpha^2]. \end{aligned} \tag{60}$$

Therefore, we can express g_{21} explicitly. Then, the following values can be computed as

$$\begin{aligned} c_1(0) &= \frac{i}{8\omega_J \tau_h}(g_{20}g_{11} - 2|g_{11}|^2 - \frac{1}{3}|g_{02}|^2) + \frac{g_{21}}{2}, \\ \mu_2 &= -\frac{Re\{c_1(0)\}}{Re\{\lambda'(2\tau_h)\}}, \\ \beta_2 &= 2Re\{c_1(0)\}, \\ T_2 &= -\frac{Im\{c_1(0)\} + \mu_2 Im\{\lambda'(2\tau_h)\}}{4\omega_J \tau_h}. \end{aligned} \tag{61}$$

Based on these parameters, we can have a relatively complete description of the bifurcated periodic solutions in the center manifold of system (1) at critical values τ_J, namely,

Theorem 3 *(i) μ_2 determines the direction of the Hopf bifurcation: if $\mu_2 > 0$ ($\mu_2 < 0$), the Hopf bifurcation is supercritical (subcritical);*
(ii) β_2 gives the stability of periodic solution: if $\beta_2 < 0$ ($\beta_2 > 0$), the periodic solution is stable (unstable);
(iii) T_2 expresses the period of the bifurcating periodic solutions: if $T_2 > 0$ ($T_2 < 0$), the period of the bifurcating periodic solution increases (decreases).

4 Exclusion of Period 3τ

We first establish the following results about the upper and lower bounds of a nontrivial positive periodic solution to system (44).

Lemma 5 *Let $y(t)$ be a nontrivial positive periodic solution of (44). Denote by m and M the minimum and maximum of $y(t)$, respectively. We have*

(i) $h((1-\alpha)y(t-\tau) + \alpha y(t-2\tau)) \le 1/e$ *for all* $t \ge 0$;
(ii) $(1-\alpha)y(t-\tau) + \alpha y(t-2\tau) \in [m, M]$ *for all* $t \ge 0$;
(iii) $me^{-M} \le h((1-\alpha)y(t-\tau) + \alpha y(t-2\tau)) \le Me^{-m}$ *for all* $t \ge 0$;
(iv) $M \le \kappa/e$;
(v) $m \le \ln\kappa \le M$.

Furthermore, if $\kappa \ge e$, we have

(vi) $me^{-m} > Me^{-M}$;
(vii) $m \ge \kappa M e^{-M}$;
(vi) $m \ge \kappa^2 e^{-1-\kappa/e}$.

Proof (i) follows from the property of function $h(x)$. (ii) is obvious. (iii) is a direct consequence of (ii). From (44) and (i), we have $\dot{y}(t) \le -y(t) + \kappa/e$. Therefore, $\limsup_{t\to\infty} y(t) \le \kappa/e$. Since $y(t)$ is periodic, we obtain $y(t) \le \kappa/e$ for all $t \ge 0$. This proves (iv). Let t_m (resp. t_M) be a minimum (resp. maximum) point of $y(t)$. Then we have $y(t_m) = m$, $y(t_M) = M$, and $\dot{y}(t_m) = \dot{y}(t_M) = 0$. Substituting these into (44) yields

$$m = \kappa h((1-\alpha)y(t_m - \tau) + \alpha y(t_m - 2\tau)), \tag{62}$$

$$M = \kappa h((1-\alpha)y(t_M - \tau) + \alpha y(t_M - 2\tau)). \tag{63}$$

In view of (iii), we obtain from the above two equations that $\kappa m e^{-M} \le m < M \le \kappa M e^{-m}$. This gives (v).

If further, $\kappa \geq e$, we will prove (vi) by contradiction. Assume to the contrary, $h(m) = me^{-m} < Me^{-M} = h(M)$. It is clear that $h((1-\alpha)y(t-\tau) + \alpha y(t-2\tau)) \geq h(m)$ for all $t \geq 0$. This together with (62) implies that $m \geq \kappa h(m) = \kappa me^{-m}$; namely, $m \geq \ln \kappa$. Since $\kappa \geq e$, we have $M > m \geq 1$. Combined the property of function $h(x)$, it then follows that $h(M) < h(m)$, a contradiction. Thus, (vi) is proved. Coupling (vi) with the following fact

$$h(x) \geq \min\{h(m), h(M)\} \quad \text{for all} \quad x \in [m, M] \tag{64}$$

gives $h((1-\alpha)y(t-\tau) + \alpha y(t-2\tau)) \geq h(M) = Me^{-M}$ for all $t \geq 0$. Substituting this into (62) implies (vii). On account of (iv) and (v), we have $\kappa/e \geq M \geq \ln \kappa \geq 1$. Since $h(x_1) > h(x_2)$ for $1 \leq x_1 < x_2$, it is easy to see that $h(M) \geq h(\kappa/e) = \kappa e^{-1-\kappa/e}$. Hence, (viii) follows from (vii).

Next, we will give a necessary condition for the existence of positive 3τ-periodic solution to system (44).

Theorem 4 *A nontrivial positive periodic solution $y(t)$ of system (44) exists only if $\max\{|h'(m)|, |h'(2)|\} \geq 2/\kappa$, where m and M are the minimum and maximum of $y(t)$, respectively.*

Proof Define $y_1(t) = y(t-\tau)$ and $y_2(t) = y(t-2\tau)$. We have a three-dimensional ordinary differential system:

$$\begin{aligned} \dot{y}(t) &= -y(t) + \kappa h((1-\alpha)y_1(t) + \alpha y_2(t)), \\ \dot{y}_1(t) &= -y_1(t) + \kappa h((1-\alpha)y_2(t) + \alpha y(t)), \\ \dot{y}_2(t) &= -y_2(t) + \kappa h((1-\alpha)y(t) + \alpha y_1(t)). \end{aligned} \tag{65}$$

The Jacobian matrix corresponding to the linear system about the periodic solution $(y(t), y_1(t), y_2(t))$ is calculated as

$$J = \begin{pmatrix} -1 & (1-\alpha)\kappa h'(Y(t)) & \alpha\kappa h'(Y(t)) \\ \alpha\kappa h'(Y_1(t)) & -1 & (1-\alpha)\kappa h'(Y_1(t)) \\ (1-\alpha)\kappa h'(Y_2(t)) & \alpha\kappa h'(Y_2(t)) & -1 \end{pmatrix}, \tag{66}$$

where $Y(t) = (1-\alpha)y_1(t) + \alpha y_2(t)$, $Y_1(t) = (1-\alpha)y_2(t) + \alpha y(t)$ and $y_2(t) = (1-\alpha)y(t) + \alpha y_1(t)$. The second additive compound matrix is given by

$$J^{[2]} = \begin{pmatrix} -2 & (1-\alpha)\kappa h'(Y_1(t)) & -\alpha\kappa h'(Y(t)) \\ \alpha\kappa h'(Y_2(t)) & -2 & (1-\alpha)\kappa h'(Y(t)) \\ (\alpha-1)\kappa h'(Y_2(t)) & \alpha\kappa h'(Y_1(t)) & -2 \end{pmatrix}. \tag{67}$$

Assume to the contrary that $\max\{|h'(m)|, |h'(2)|\} < 2/\kappa$. Due to $|h'(x)| \leq \max\{|h'(m)|, |h'(2)|\}$ for all $x \geq m > 0$, it follows that $|\kappa h'(Y(t))| < 2$, $|\kappa h'(Y_1(t))| < 2$ and $|\kappa h'(Y_2(t))| < 2$. Thus, the Lozinskii measure $\mu(J^{[2]})$ is negative. By Li and Muldowney[21], the system (65) has no periodic solution. This leads to a contradiction. Therefore, we must have $\max\{|h'(m)|, |h'(2)|\} \geq 2/\kappa$.

Thus, we get the following result for the nonexistence of positive $3\tilde{\tau}$-periodic solution to (44).

Corollary 1 *If $\kappa \leq 11$, then equation (44) has no positive $3\tilde{\tau}$-periodic solution.*

Proof First, one can prove that when $\kappa < e$, there is no positive equilibrium or periodic solution for the delay differential equation (44). Next, we consider the case $e \le \kappa \le 11$. Assume to the contrary that $y(t)$ is a $3\tilde{\tau}$-periodic solution to (44) with maximum M and minimum m. By Lemma 5 (viii), we have $m \ge \kappa^2 e^{-1-\kappa/e} \ge 11^2 e^{-1-11/e} \ge 0.7$. Therefore, we obtain $\max\{|h'(m)|, |h'(2)|\} \le \max\{|h'(0.7)|, |h'(2)|\} \le 0.15$. However, Theorem 4 implies $\max\{|h'(m)|, |h'(2)|\} \ge 2/p \ge 2/11 \ge 0.18$, a contradiction.

Summarizing the discussion, we have the following sufficient condition for nonexistence of positive 3τ-periodic solution to system (1):

Theorem 5 *If $\rho r/d \le 11$, then equation (1) has no positive 3τ-periodic solution.*

5 Global Continuation of Periodic Solutions

We now engage the global Hopf bifurcation theorem to establish the existence of global continuation of periodic solutions for $\tau = \tau_J$.

Note that when $\tau = \tau_J$ there exists a Hopf bifurcation of periodic solution at x_+^* for model (1) with period $2\pi/\omega_J$. To use the global bifurcation theorem of Erbe et al. (1992), we need to reformulate the bifurcation problem in a functional analytical setting. We make the change of variable $y(t) = x(t/\omega)$ so that model (1) can be transformed as

$$y'(t) = \frac{1}{\omega}[-dy(t) + f((1-\alpha)\rho y(t-\omega\tau) + \alpha\rho y(t-2\omega\tau))] \tag{68}$$

and $y(t)$ is a 2π-periodic solution of (68) if and only if $x(t)$ is a $2\pi/\omega$-periodic solution of (1). This allows us to transform the problem of searching for a periodic solution of (1) with bifurcation parameter(τ)-dependent period to the problem of searching for a periodic solution of (68) with a fixed period 2π. However, (68) becomes a parameterized DDE with two parameters, ω and τ.

Recall that the characteristic equation of model (1) is $\Delta(\Lambda, \tau) = 0$. We have shown in Sect. 2.2 the isolated centers of the analytic function $\Delta(\Lambda, \tau) = 0$ are given by $(i\omega_J, \tau_J)$. We can also find $\delta > 0$ such that the closure of $\Omega = (0, \delta) \times (\omega_J - \delta, \omega_J + \delta)$ contains no other zeros of $\Delta(\Lambda, \tau)$. Therefore, we can define

$$\gamma_{\tau_J \pm} := \deg_B(\Delta(\cdot, \tau_J \pm \delta), \Omega) \tag{69}$$

with $\deg_B$ being the Brouwer degree of the analytic function $\Delta(\cdot, \tau_J \pm \delta)$ with respect to Ω, and the so-called crossing number is defined as

$$\gamma_{\tau_J} := \gamma_{\tau_J -} - \gamma_{\tau_J +}. \tag{70}$$

From Theorem 2, we have

Corollary 2 $\gamma_{\tau_J} = -1$.

Let $E \times \mathbb{R} \times \mathbb{R}^+$ be the Fuller space, where E is the Banach space of 2π-periodic functions equipped with the sup-norm. $\gamma_{\tau_J} \ne 0$ implies that $(x_+^*, \tau_J, \omega_J)$ is a bifurcation point in the sense that near $\tau = \tau_J$. (1) has a non-constant periodic solution near x_+^* with period $2\pi/\omega_J$, so there is a nonempty connected component of this bifurcation in $\sum$, the closure of the set of all nontrivial periodic solutions of (68) in $E^+ \times \mathbb{R}^+ \times \mathbb{R}^+$. Here E^+ is the open set of continuous positive 2π-periodic functions.

We now notice that the operator for any $\omega > \tilde{\omega}^*$ and $\tau \geq 0$, $F : E^+ \times \mathbb{R}^+ \times \mathbb{R}^+ \to E$ defined by

$$F(y, \tau, \omega)(t) = \frac{1}{\omega}[-dy(t) + f((1-\alpha)\rho y(t-\omega\tau) + \alpha\rho y(t-2\omega\tau))], \quad t \in R, \tag{71}$$

satisfies a global Lipschitz condition:

$$|F(y, \tau, \omega) - F(\tilde{y}, \tau, \omega)|_{t\in R} \leq \left(\frac{d}{\tilde{\omega}^*} + \rho L_f\right)|y(t) - \tilde{y}(t)|_{t\in R} \tag{72}$$

for any $y, \tilde{y} \in E^+$, where L_f is the global Lipschitz constant for the function $f : [0, +\infty) \to [0, +\infty)$ defined by (2).

A stationary point of (68) is (y, τ, ω) with y being a constant such that

$$-dy + f(\rho y) = 0. \tag{73}$$

As we know this equation has only one positive equilibrium $y^* = x_+^*$ and a zero equilibrium 0, so the only stationary points of (68) in $\mathrm{Cl}\{(y, \tau, \omega) \in E^+ \times \mathbb{R}^+ \times \mathbb{R}^+\}$ are $(0, \tau, \omega)$ and (x_+^*, τ, ω).

From Sect. 4, it is easy to prove that nontrivial nonnegative periodic solutions of equation (68) have a uniform positive lower bound m and a uniform positive upper bound M. Therefore, the projection of $\sum$ onto the E^+ space is bounded by m and M from below and above. The intersection of $\sum$ with the set of stationary points is only $\{(x_+^*, \tau, \omega), \tau \in \mathbb{R}^+, \omega \in \mathbb{R}^+\}$.

Note that for the fixed $\alpha \in (\max(-\frac{d}{\rho f'(\rho x_+^*)}, \frac{1}{2}), 1)$, the minimal τ such that the linearization at x_+^* of model (1) has a pair of purely imaginary characteristic values is $\tau = \tilde{\tau}^*$. The intersection of $\sum$ with the set of trivial solutions of (68) is $(x_+^*, \tau_J, \omega_J)$. From Theorem 5 and condition (41), we can show that the period $\frac{2\pi}{\omega}$ is bounded from below and above, namely,

$$3\tau < \frac{2\pi}{\omega} < 6\tau. \tag{74}$$

Then applying the global Hopf bifurcation theorem [13] to the $\mathrm{Cl}\{E^+ \times (0, \infty) \times (0, \infty)\}$, we conclude that the projection of $\sum$ onto the τ-space must be $[\tilde{\tau}^*, \infty)$. Therefore, we have the following result:

Theorem 6 *Assume* $\frac{\rho r}{d} \leq 11$ *holds. For any* $\alpha \in \left(\max\left(-\frac{d}{\rho f'(\rho x_+^*)}, \frac{1}{2}\right), \min\left(\frac{1}{2} - \frac{d}{\rho f'(\rho x_+^*)}, 1\right)\right)$, *there exists* τ^* *calculated in* (14) *such that for any* $\tau \in (\tau^*, +\infty)$ *equation* (1) *has a non-constant periodic solution oscillating around* x_+^* *with a period in* $(3\tau, 6\tau)$.

6 Numerical Bifurcation Analyses

We now present some numerical experiments to demonstrate the onset and global continuation of Hopf bifurcations for the considered system (1) with some parameters collected from published literature: $d = 1$; $\rho = 0.0081$; $r = 1180$; $\sigma = 0.001$; $\alpha = 0.8644$.

We can then calculate the positive equilibrium value $x_+^* = 27877$ of model (1), and concluded that the linearization at this positive equilibrium has a pair of purely imaginary

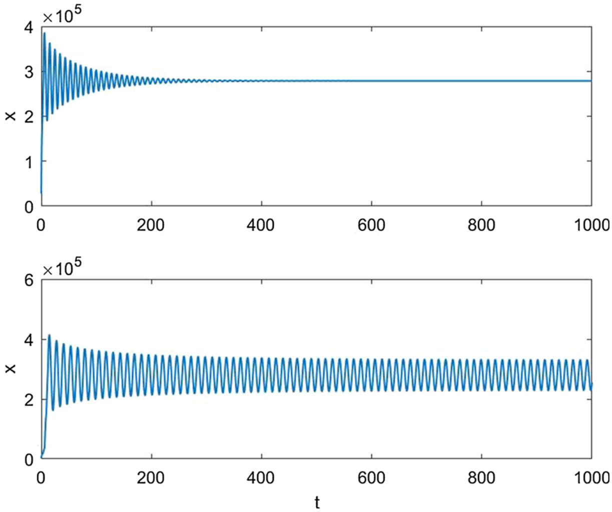

Fig. 4 The positive equilibrium x_+^* is asymptotically stable when $\tau = 2(< \tau^*)$ and becomes unstable when $\tau = 2.9(> \tau^*)$, leading to a Hopf bifurcation of periodic solutions

eigenvalues $\pm i\omega$, where $\omega = 1.4055$. Furthermore, we can calculate the critical value of delay $\tau^* = 2.703$. From the top panel of Fig. 4, it is easy to observe that the positive equilibrium x_+^* is asymptotically stable when $\tau < \tau^*$, while the bottom panel of Fig. 4 shows that x_+^* loses stability and a Hopf bifurcation occurs when $\tau > \tau^*$. Based on the algorithm derived from Sect. 3, we can also calculate the following values: $c_1(0) = -0.2359 - 0.0354i$, $\lambda'(2\tau^*) = 0.0481 - 0.2611i$, $\mu_2 = 4.9044$, $\beta_2 = -0.4717$ and $T_2 = 0.0866$. Therefore, by Theorem 3, we conclude that model (1) undergoes a supercritical Hopf bifurcation at the positive equilibrium x_+^* and the bifurcating periodic solutions are stable.

We note that when $\alpha = 0$, the first critical value of the delay when the linearization of mode (1) at the positive equilibrium x_+^* has a pair of purely imaginary eigenvalues is 4.08 which is larger than $\tau^* = 2.703$. The biologically realistic range for the normal development delay is between 2 and 3 years. Therefore, in this biologically realistic range, the model system (1) without diapause can not exhibit periodic oscillations around the positive equilibrium.

We have also applied the pseudospectral approximation of delay equations developed in [6] to generate an ODE system (with dimension 21) and using the Matlab package MatCont [9] to generate some numerical Hopf bifurcation plots. In particular, Fig 5 illustrates the onset and global continuation of Hopf bifurcations with respect to τ using equilibrium (solid stable and dashed unstable) and the min/max value of periodic solutions. Hopf bifurcation is detected at $\tau \approx 2.7$, corresponding to the pair of eigenvalues $\pm 0.52i$. No bifurcation was detected on the branch of periodic solutions. We also plotted the ratio period/delay of the periodic solutions by varying τ in the given interval. It is clear that this ratio is bounded by 3 from below and 6 from above, to numerically illustrate the theoretical result that excludes periodic solutions of period 3τ.

Our normal form calculations have confirmed that the bifurcated periodic solutions are stable when the delay is near the critical value. The pseudospectral approximation of delay equations allows us to approximate the Floquet multipliers of the bifurcated periodic solutions from calculating the multipliers of the approximating ODE system to conclude the stability of bifurcated periodic solutions along the global continuation. Fig. 6 gives the periodic orbits

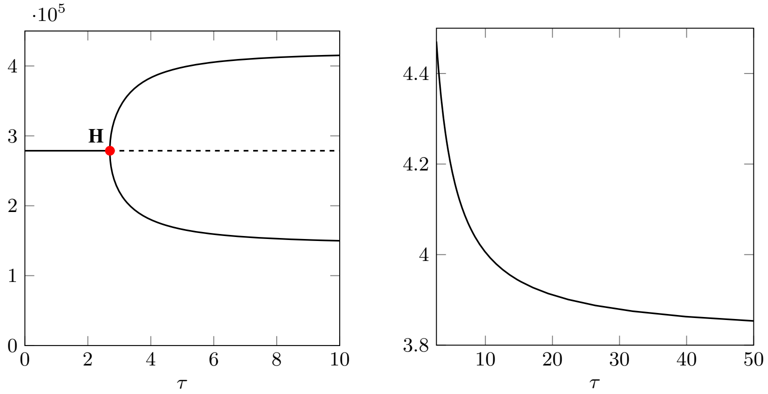

Fig. 5 (Left panel) A global Hopf bifurcation diagram with respect to τ, using equilibrium (solid stable and dashed unstable) and the min/max value of periodic solutions. Hopf bifurcation is detected at $\tau \approx 2.7$ with corresponding pair of eigenvalues $\pm 0.52i$. No bifurcation was detected on the branch of periodic solutions. (Right panel): Ratio of period/delay of the periodic solutions with respect to $\tau \in (\tau^*, 50)$

(within the periods) and the location of the first few Floquet multipliers: top panel for $\tau \approx 2.7$, with period $p \approx 12.07$; while bottom panel for $\tau = 10$, with period $p \approx 40.05$. It remains an interesting topics to see if this pseudospectral approximation of delay equations by an ODE system can give results, similar to those on the persistence of periodic solutions under perturbations in dynamical systems generated by evolutionary equations [17].

7 Discussion

Tick-borne diseases are mainly transmitted and maintained in the tick-host enzootic cycle, but human can also be infected through the bites of infected ticks. Climate change has been facilitating the transmission both within the enzootic cycle and to the human [1,7,28]. So understanding tick population dynamics is important for the prevention and control of tick-borne diseases [4,12,22].

An important mechanism for ticks to adapt to climate variation for survival is diapause, development activity suspension. Explicitly incorporating diapause into a model formulation of tick population dynamics leads naturally to a delay differential system with multiple delays. Here, we consider a model that takes into account of two types of diapause, behavioural diapause for unfed ticks and developmental diapause for engorged ticks. The model we considered assumes that diapause occurs in every stage of tick's life cycle once egg-hatching lags behind seasonal climatic rhythm. Specially, we consider the case where hatching-eggs, engorged larvae and nymphs undergo developmental diapause, and questing larvae, questing nymphs and questing adults enter behavioural diapause. Based on some laboratory observations [10,16,36], ticks experiencing diapause will spend 4–6 years to complete their lifecycle which is approximately twice of the period of normal developing life span. In this way, we have obtained a delay differential equation with two delays where diapause delay doubles the normal development duration. In addition to the references cited in the introduction section, we note that the Hopf bifurcation analyses are always complicated for delay differential equations with multiple delays, even these delays are rationally related [5,18,23].

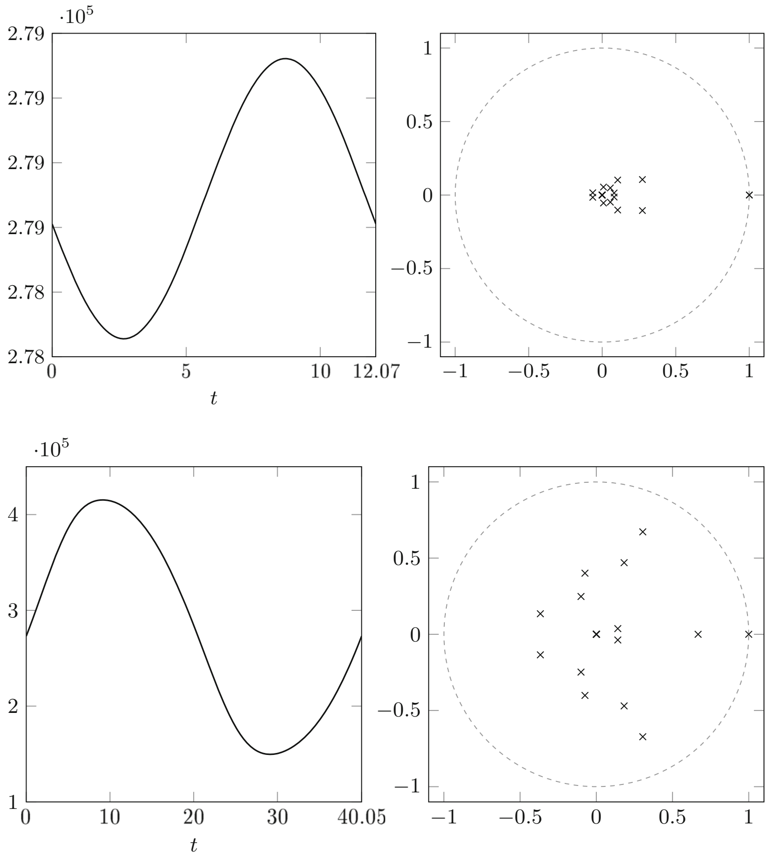

Fig. 6 Variations of periodic orbits and their Floquet multipliers when τ increases from the critical value τ^*: top panel corresponds to τ near τ^*, and bottom panel for $\tau = 10$

Here, we used the normal development delay, τ, as a Hopf bifurcation parameter, to examine the onset and global continuation of Hopf bifurcations of periodic solutions. In Sects. 2 and 3, we found explicitly (thanks to the description of the monotonicity of parametric tangent functions) the first critical bifurcation value of τ and determined the direction of Hopf bifurcation and stability of periodic solutions bifurcation from the positive equilibrium x_+^* through normal form and center manifold calculations. We then show this Hopf bifurcation has an unbounded component after checking the crossing number at every possible Hopf bifurcation point and using the S^1-degree based global Hopf bifurcation theory. After the utilization of the Muldoney-Li technique for exclusion of periodic solutions with period 3τ, we showed that the Hopf bifurcation has a global continuation with its projection onto the τ-space unbounded. This ensures the existence of large-amplitude periodic solutions for all τ exceeding the first bifurcation value.

We anticipate this work can be extended in many different ways. A first step is to add explicitly the disease transmission, expanding the ecological model to an epidemic model. The next step is to incorporate explicit temperature variation, this will lead to a periodic or a quasi-periodic system with multiple delays.

Acknowledgements This research has been supported by the Natural Science Foundation of China (No. 11701072), the NSERC/Sanofi Industrial Research Chair program in "Vaccine Mathematics, Modelling and Manufacturing"; the GlaxoSmithKline's Investigator Sponsored Studies "Estimating risk of tick-borne encephalitis with changes in climate, habitation and recreational activities", the Canada Research Chairs program and the Natural Sciences and Engineering Research Council of Canada.

References

1. Alkishe, A.A., Peterson, A.T., Samy, A.M.: Climate change influences on the potential geographic distribution of the disease vector tick Ixodes ricinus. PLoS ONE **12**(12), e0189092 (2017)
2. Belozerov, V.N.: Diapause and the conditions for the reactivation of females of the tick Dermacentor marginatus Sulz (Ixodidae). Vest. Leningr. Univ. Leningrad **1**, 5–11 (1964)
3. Belozerov, V.N.: New aspects in investigations of diapause and non-diapause dormancy types in insects and other arthropods. Entomol. Rev. **89**(2), 127–136 (2009)
4. Belozerov, V.N., Naumov, R.L.: Nymphal diapause and its photoperiodic control in the tick Ixodes scapularis (Acari: Ixodidae). Folia Parasitol. **49**, 314–318 (2002)
5. Braddock, R.D., van den Driessche, P.: A population model with two time delays. In: Chapman, D.G., Gallucci, V.F. (eds.) Quantitative Population Dynamics. Statistical Ecology Series, vol. 13. International Cooperative Publishing House, Fairland (1981)
6. Breda, D., Diekmann, O., Gyllenberg, M., Scarabel, F., Vermiglio, R.: Pseudospectral discretization of nonlinear delay equations: new prospects for numerical bifurcation analysis. SIAM J. Appl. Dyn. Syst. **15**(1), 1–23 (2016)
7. Dantas-Torres, F.: Climate change, biodiversity, ticks and tick-borne diseases: the butterfly effect. Int. J. Parasitol. Parasites Wildl. **4**(3), 452–461 (2015)
8. Dantas-Torres, F., Chomel, B.B., Otranto, D.: Ticks and tick-borne diseases: a one health perspective. Trends Parasitol. **28**, 437–446 (2012)
9. Dhooge, A., Govaerts, W., Kuznetsov, YuA, Meijer, H.G.E., Sautois, B.: New features of the software MatCont for bifurcation analysis of dynamical systems. MCMDS **1**(2), 147–175 (2008)
10. Diyes, G.C.P., Rajakaruna, R.S.: Life cycle of Spinose ear tick, Otobius megnini (Acari: Argasidae) infesting the race horses in Nuwara Eliya, Sri Lanka. Acta Trop. **166**, 164–176 (2017)
11. Dobson, A.D.M., Finnie, T.J.R., Randolph, S.E.: A modified matrix model to describe the seasonal population ecology of the European tick Ixodes ricinus. J. Appl. Ecol. **48**(4), 1017–1028 (2011)
12. Dunn, J.M., Davis, S., Stacey, A., Diuk-Wasser, M.A.: A simple model for the establish of tick-borne pathogens of Ixodes scapularis: a global sensitivity analysis of R0. J. Theor. Biol. **335**, 213–221 (2013)
13. Erbe, L.H., Geba, K., Krawcewicz, W., Wu, J.: Sl-degree and global Hopf bifurcation theory of functional differential equations. J. Differ. Equ. **98**, 277–298 (1992)
14. Estrada-Peña, A., de la Fuente, J.: The ecology of ticks and epidemiology of tick-borne viral diseases. Antivir Res. **108**, 104–128 (2014)
15. Gakkhar, S., Singh, A.: Complex dynamics in a prey predator system with multiple delays. Commun. Nonlinear Sci. Numer. Simul. **17**(2), 914–929 (2012)
16. Gray, J.S., Kahl, O., Lane, R.S., Levin, M.L., Tsao, J.I.: Diapause in ticks of the medically important Ixodes ricinus species complex. Ticks Tick Borne Dis. **7**(5), 992–1003 (2016)
17. Hale, J.K., Raugel, G.: Persistence of periodic orbits for perturbed dissipative dynamical systems. In: Mallet-Paret, J., Wu, J., Yi, Y., Zhu, H. (eds.) Infinite Dimensional Dynamical Systems. Fields Institute Communications, vol. 64, pp. 1–55. Springer, New York (2013)
18. Hale, J.K., Huang, W.: Global geometry of the stable regions for two delay differential equations. J. Math. Anal. Appl. **178**, 344–362 (1993)
19. Hassard, B.D., Kazarinoff, N.D., Wan, Y.H.: Theory and Applications of Hopf Bifurcation. Cambridge University Press, Cambridge (1981)
20. Li, M.Y., Wang, C., Wei, J.: Global Hopf bifurcation analysis of a Nicholson's Blowflies equation of neutral type. J. Dyn. Differ. Equ. **26**, 165–179 (2014)
21. Li, Y., Muldowney, J.S.: On Bendixson's criterion. J. Differ. Equ. **106**(1), 27–39 (1993)
22. Lou, Y., Wu, J., Wu, X.: Impact of biodiversity and seasonality on Lyme-pathogen transmission. Theor. Biol. Med. Model. **11**(1), 50 (2014)
23. Mahaffy, J.M., Busken, T.C.: Regions of stability for a linear differential equation with two rationally dependent delays. Discrete Continuous Dyn. Syst. **35**(10), 4955–4986 (2015)
24. Mallet-Paret, J., Nussbaum, R.D.: A differential-delay equation arising in optics and physiology. SIAM J. Math. Anal. **20**(2), 249–292 (1989)

25. Marquardt, W.C.: Biology of Disease Vectors, 2nd edn. Elservier Academic Press, Burlington (2005)
26. Mendy, A., Tewa, J.J., Lam, M., Tchinda Mouofo, P.: Hopf bifurcation in a grazing system with two delays. Math. Comput. Simul. **163**, 90–129 (2019)
27. Milne, A.: The ecology of the sheep tick, Ixodes ricinus L. Host availability and seasonal activity. Parasitology **36**, 153–157 (1945)
28. Oliveira, S.V., Gazeta, G.S., Gurgel-Gonçalves, R.: Climate, ticks and tick-borne diseases: mini review. Vector Biol. J. **2**(1), 1–3 (2017)
29. Ricker, W.E.: Computation and Interpretation of Biological Statistics of Fish Populations. Bull Fish Res Board Can No. 191. Blackburn Press, Ottawa (1975)
30. Rosendale, A., Dunlevy, M., Fieler, A., Farrow, D., Joshua, B., Benoit, B.: Dehydration and starvation yield energetic consequences that affect survival of the American dog tick. J. Insect Physiol. **101**, 39–46 (2017)
31. Shayer, L.P., Campbell, S.A.: Stability, bifurcation, and multistability in a system of two coupled neurons with multiple time delays. SIAM J. Appl. Math. **61**, 673–700 (2000)
32. Smith, H.: Monotone Dynamical Systems, an Introduction to the Theory of Competitive and Cooperative Systems. Mathematical Surveys and Monographs. American Mathematical Society, Providence (1995)
33. Song, P., Xiao, Y.: Global hopf bifurcation of a delayed equation describing the lag effect of media impact on the spread of infectious disease. J. Math. Biol. **76**(5), 1249–1267 (2018)
34. Song, P., Xiao, Y.: Analysis of an epidemic system with two response delays in media impact function. B. Math. Biol. **81**(5), 1582–1612 (2019)
35. Sun, X., Wei, J.: Stability and bifurcation analysis in a viral infection model with delays. Adv. Differ. Equ. **332**, 1–22 (2015)
36. Walker, A.R.: Age structure of a population of Ixodes ricinus (Acari: Ixodidae) in relation to its seasonal questing. B. Entomol. Res. **91**, 69–78 (2001)
37. Wang, L., Niu, B., Wei, J.: Dynamical analysis for a model of asset prices with two delays. Phys. A. **447**, 297–313 (2016)
38. Yang, H., Wei, J.: Note on the stability of reaction-diffusion systems with delays by Lyapunov functional. Appl. Math. Lett. **83**, 151–155 (2018)
39. Zhang, X., Wu, J.: Critical diapause portion for oscillations: parametric trigonometric functions and their applications for Hopf bifurcation analyses. Math. Methods Appl. Sci. **42**(5), 1363–1376 (2019)